

# Microplastic Lens Array Fabricated by a Hot Intrusion Process

Li-Wei Pan, *Member, IEEE*, Xinjiang Shen, and Liwei Lin, *Member, IEEE, Member, ASME*

**Abstract**—A microplastic lens array has been successfully constructed on top of a 500- $\mu\text{m}$ -thick PC (Polycarbonate film) by using a micro hot intrusion process. A single-layer LIGA process is used to fabricate the high-aspect-ratio nickel mold insert that has circular hole patterns of 80  $\mu\text{m}$  in diameter and 200  $\mu\text{m}$  in depth. Under the hot intrusion process, plastic material can be intruded into these circular-shape holes and stopped at desired depth under elevated temperature and pressure to fabricate microlenses. By adjusting the embossing load, temperature and time, the curvature and height of the lens are controllable when the same mold insert is used. The optical properties of these microlenses have been characterized and the average radius of curvature is found as 41.4  $\mu\text{m}$  with a standard deviation of 1.05  $\mu\text{m}$ . Experimental characterization and theoretical model are conducted and developed for the micro-intrusion process in terms of the radius of curvature and height of the lenses and they correspond well with experimental data within 5% of variations. The focusing capability of the lenses is demonstrated by comparing the images of laser light with and without using the lenses. When the projection screen is placed 200  $\mu\text{m}$  away from the lens, the full-width at half-maximum (FWHM) for the lens is 110  $\mu\text{m}$  while the original FWHM of the optical fiber is 300  $\mu\text{m}$ . [1201]

**Index Terms**—Contactless, microintrusion, microlens, lens.

## NOMENCLATURE

T	Temperature.
f	Focal length.
f/#	f-number.
t	Time.
h	Height.
R	Radius of curvature.
n	Reflection index.
D	Diameter of the circular opening.
C	Constant.
G	Universal gas constant.
$\Delta H$	Activation energy.
P	Pressure
$\theta$	Contact angle.

Subscript:  
air Air.

Manuscript received November 17, 2003; revised March 25, 2004. This work was supported in part by an NSF Award (DMI-0096220) and by DARPA Grant under the MTO/MEMS program. This paper was presented in part at the IEEE Micro Electro Mechanical Systems Conference, Orlando, FL, Jan. 17–21, 1999 and the Transducers'01/Eurosensors XV Conference, Munich, Germany, June 10–14, 2001. Subject Editor E. Obermeier.

L.-W. Pan is with Perkin Elmer, Inc., Santa Clara, CA 95054 (e-mail: li-wei.pan@perkinelmer.com).

X. Shen and L. Lin are with the Mechanical Engineering, University of California at Berkeley, CA 94720 USA.

Digital Object Identifier 10.1109/JMEMS.2004.838363

p	Plastic.
R	Curvature.
M	Focus at M.
L	Focus at L.
$\sigma$	Microlens apex to the top surface of mold insert steady-state.

## I. INTRODUCTION

MICROLENSSES are key elements in optical microsystems and the majority of them are made of plastic materials in common MEMS (Microelectromechanical Systems) applications. Previously, attempts were made to fabricate three-dimensional (3-D) lenses with different micromachining techniques, including lithographic methods [1], [2], reflow of photoresist [3] and isotropic etching of silicon as mold inserts for the plastic molding processes [4], [5]. Surface roughness and the controllability of radius of curvature of the microlens are two major engineering challenges. Particularly, both the lithographic method and reflow of the photoresist could be difficult to control such that the curvature of the lens may vary on the same wafer and from one process run to another. On the other hand, the conventional plastic molding process might have problems in the flatness control of the lens surface due to possible defects on the mold inserts. In practice, the resist reflow process can control the lens height on the order of 2–4% across a large array [6] and others also report excellent results from various manufacturing methodologies [7]–[9].

This paper introduces a micro-intrusion process that has been developed and modified from a microhot-embossing process [10]–[12] as an alternative way to make plastic microlenses. By adjusting the processing temperature, pressure and time, the radius of curvature and height of the microlens could be controlled. Furthermore, the top hemispherical portion of the microlens is naturally constructed by the intrusion of plastic material without touching any mechanical parts. Therefore, microlens with fine surface and desirable radius of curvature can be fabricated for optical applications.

## II. THE MICRO INTRUSION PROCESS

The process flow of the micro intrusion process is illustrated in Fig. 1. First, a standard LIGA process is used to make the mold inserts. In the prototype demonstration, these molds are provided by MCNC [13] to make nickel mold insert with circular openings of 80  $\mu\text{m}$  in diameter and of the depth of the mold insert is 200  $\mu\text{m}$ . A sheet of PC (Polycarbonate) film of 500  $\mu\text{m}$  in thickness is placed underneath the mold insert as

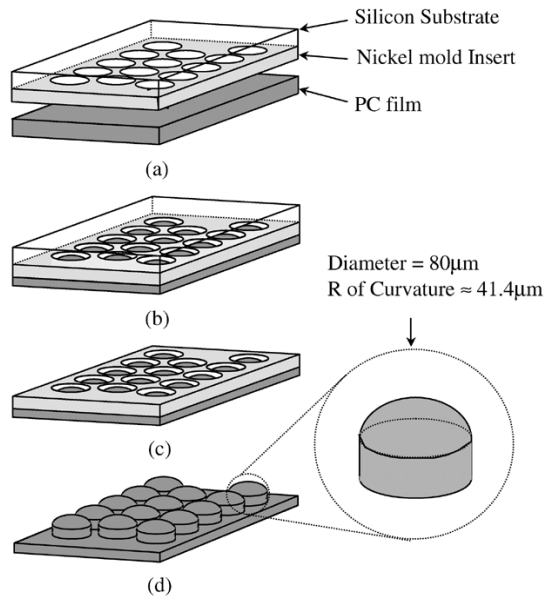


Fig. 1. Fabrication sequences of the microhot intrusion process: (a) mold insert and polycarbonate film, (b) microhot intrusion under elevated temperature and pressure, (c) release of the silicon substrate if an LIGA mold insert is used, and (d) release of plastic lenses.

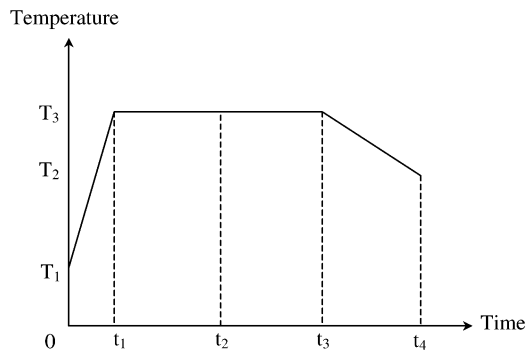


Fig. 2. The temperature and time sequence during the micro-intrusion process.  $T_1$  is the room temperature,  $T_2$  is the demolding temperature, and  $T_3$  is the hot intrusion process temperature. Before  $t_2$ , a preload is applied. Between  $t_2$  and  $t_3$ , the intrusion of plastic material occurs. After  $t_3$ , the external pressure is still applied in the demolding process.

shown in Fig. 1(a). They are pressed firmly at an elevated temperature that is higher than the glass transition temperature of the PC film (140 °C to 150 °C). When an adequate pressure is applied, the plastic material deforms and intrudes into the circular openings as shown in Fig. 1(b). At the end of the process, the silicon substrate that comes with the LIGA mold insert can be released by etching the seed layer on the LIGA substrate as illustrated in Fig. 1(c) for further processing or the plastic microlenses can be demolded as shown in Fig. 1(d).

Fig. 2 shows the temperature and processing time sequences at various steps of the process. The temperature is first raised from room temperature,  $T_1$ , to a desired processing temperature,  $T_3$ , which should be higher than the glass transition point of the plastic material. The heating rate is about 10 °C per minute in this prototype demonstration. During this step, a small force of 100 Newton (about 0.1 MPa of pressure on a molding

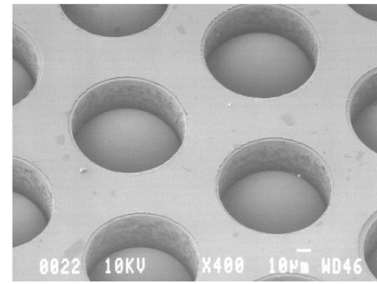


Fig. 3. SEM of the microlens (from the 80  $\mu$ m in diameter mold insert) array with the nickel mold insert at the completion of step (c) in Fig. 1.

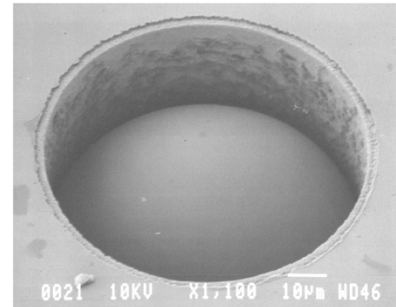


Fig. 4. The close view of Fig. 3 showing a single microlens (from the 80  $\mu$ m in diameter mold insert) with the nickel mold insert still in tact.

area of 1  $\text{cm}^2$ ) is applied to maintain the contact between the PC film and nickel mold insert. The load and temperature are then kept constant for about 20 min when  $t_2$  as marked in Fig. 2 is reached. At this moment, the processing load (0.3 MPa to 1.3 MPa) is applied and held for 20 min until  $t_3$  is reached. This is the most crucial stage that plastic material flows and intrudes inside the nickel mold insert to microlenses are formed. The temperature is then reduced to a demolding temperature,  $T_2$ , which is set at 80 °C and the cooling rate is set at 4 °C/minute. It is desirable to keep this cooling rate as slow as possible to reduce thermal stresses. The processing load should be kept on the samples during this cooling step to reduce possible shrinkage of PC film. When the temperature reaches,  $T_2$ , as marked as  $t_4$  in the time axis in Fig. 2, the samples are taken out of the machine and the micro-intrusion process is completed.

Fig. 3 shows the fabricated microlens array with nickel mold insert after they are released from the silicon substrate. In this case, the nickel mold insert is still intact and the separation distance between the edges of two lenses is 40  $\mu$ m. A close view scanned electron micrograph (SEM) in Fig. 4 shows that the sidewall of the nickel mold insert is actually pretty rough as the result of the electroplating process [13]. However, the naturally formed lens surface on the top is smooth as shown. Our previous characterizations on hot embossed microstructures using AFM (Atomic Force Microscope) indicate that the average surface roughness of hot embossed polymer structures is 1–4 nm [14] and would qualify for optical applications. A wholly demolded microlens can be seen in Fig. 5, where a tiny trace along the interface of the lens and the cylindrical column is identified. This imperfection line is probably caused by the intersection of the intruded plastic material and the rough nickel mold insert during the micro intrusion process.

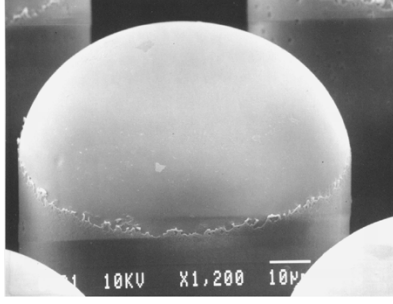


Fig. 5. SEM of a microlens (from the 80  $\mu\text{m}$  in diameter mold insert) after the demolding process representing the completion of step (d) in Fig. 1.

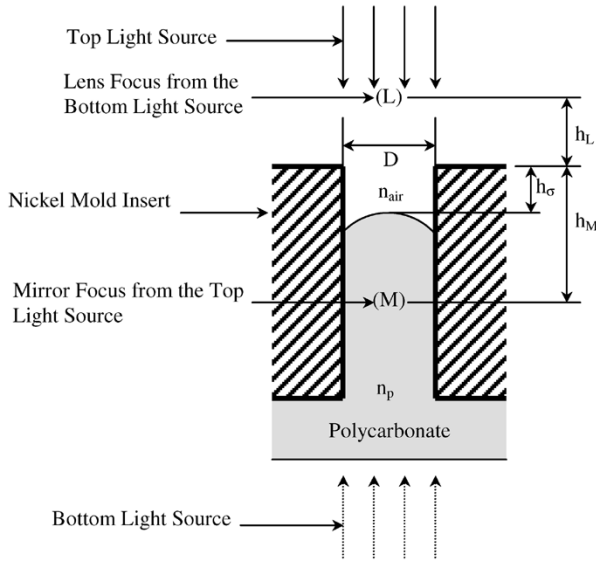


Fig. 6. The schematic diagram showing the scheme to measure radius of curvature of microlenses by measuring foci from both top and bottom light sources.

### III. EXPERIMENTAL CHARACTERIZATIONS

#### A. Radius of Curvature of the Microlenses

In order to characterize the optical properties of the microlenses, a microscope that has dual light sources from both the top and bottom of the sample (coated with a thin gold layer for SEM) is used to find the two foci as illustrated in Fig. 6 with corresponding parameters. When the light is emitting from the top and reflected, a focus can be found at a position inside the plastic microlens. A focus/defocus scheme (focusing on the focal point of the microlens first, and then focusing on the top surface of the nickel mold insert, and noting the distance from these two positions from the scale reading on the optical microscope) is used to measure the distance,  $h_M$ , between the top surface of the nickel insert and the focus, (M). When the light is emitting from the bottom of the microlens, a focus can be observed above of the lens and is denoted as (L), as shown in Fig. 6. The same focus/defocus measurement scheme is applied to determine the distance,  $h_L$ , between the top surface of the

nickel mold insert and the focus. Two fundamental optical and geometrical equations [15], [16] are derived

$$\frac{1}{h_M - h_\sigma} = \frac{2}{R} \quad (1)$$

$$\frac{n_{\text{air}}}{h_L + h_\sigma} = \frac{(n_p - n_{\text{air}})}{R}. \quad (2)$$

As illustrated in Fig. 6,  $R$  is the radius of curvature of the microlenses,  $h_\sigma$  is the distance between the microlens apex and the top surface of the nickel mold insert.  $D$  is the diameter of the circular opening on the nickel mold insert, and  $n_{\text{air}}$  and  $n_p$  are the refractive index of air and the PC film, respectively.

The two unknowns,  $R$  and  $h_\sigma$  can be solved by the above two equations and the lens curvature  $R$  can be represented as

$$R = \frac{2(n_p - n_{\text{air}})}{n_{\text{air}} + n_p} (h_L + h_M) \quad (3)$$

The radii of curvature of 48 microlenses (in a  $6 \times 8$  array, within an area of  $800 \times 1000 \mu\text{m}^2$ ) from a single process run are measured as shown in the histogram in Fig. 7. The average radius of curvature is 41.4  $\mu\text{m}$  with a standard deviation of 1.05  $\mu\text{m}$ . The  $f$ -number,  $f/\#$ , or the inverse of the relative aperture can be calculated as

$$f/\# = \frac{f}{D} \quad (4)$$

where  $D$  is the diameter of the opening hole and  $f$  is the focal length as derived as

$$\frac{n_{\text{air}}}{f} = \frac{(n_p - n_{\text{air}})}{R}. \quad (5)$$

In the prototype demonstration, one side of the microlens is flat and the refractive index of the PC material is 1.58 such that the average focal length is 70.7  $\mu\text{m}$  and the average  $f/\#$  is 0.88.

#### B. Experimental Demonstration

An optical system is setup for the experimental demonstration as shown in Fig. 8. The light source is a 623.8 nm He-Ne laser. A single mode optical fiber is first aligned with the laser beam by using a micromanipulator. The other end of the fiber is aligned with one microlens with the help of a second micromanipulator. The microlens array is fixed on the chuck stage of a probe station underneath a projection screen, which is aligned with the microscope with the help of a third micromanipulator. The distance between the microlens and the projection screen is about 200  $\mu\text{m}$ . The focused image is then taken by a charge-coupled device (CCD) camera via the objective lens on the probe station. Fig. 9 shows the measured images and relative intensity from the optical fiber with (left) and without (right) using the microlenses.

The intensity distribution of each case is converted from the image by MATLAB [17]. The FWHM of each case is measured from the relative intensity distribution with an original value of 300  $\mu\text{m}$  for the optical fiber and 110  $\mu\text{m}$  with the assistance of the microlenses.

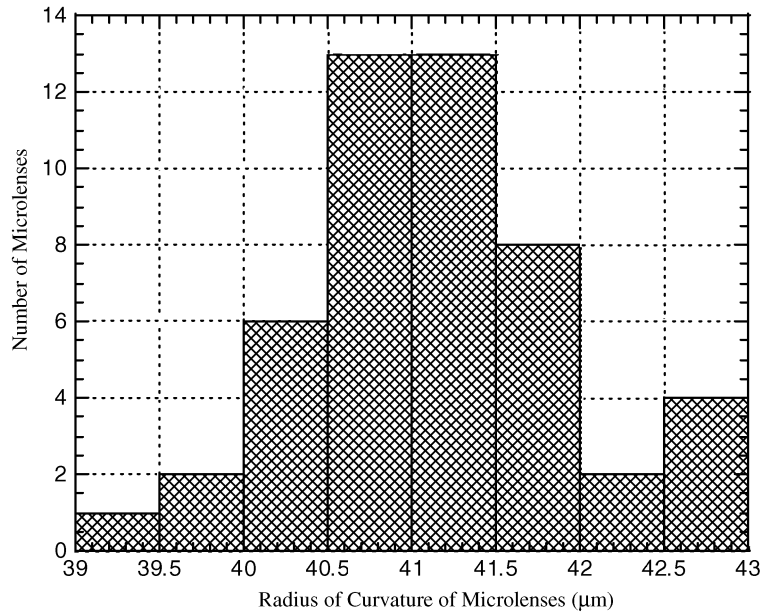


Fig. 7. Histogram of the radius of curvature of microlenses ( $80 \mu\text{m}$  in diameter) indicates good controllability of the micro-intrusion process.

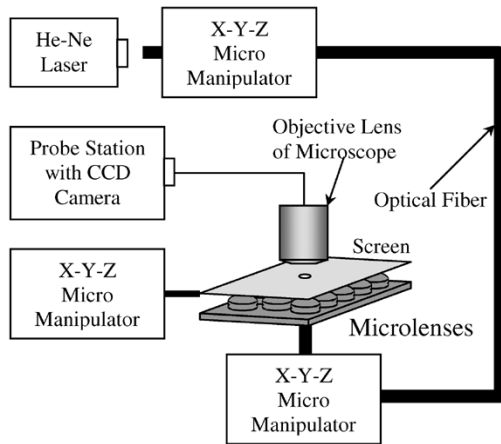


Fig. 8. The schematic diagram of the focusing experiment using a He-Ne laser and optical fiber.

#### IV. DISCUSSIONS

The above optical properties are measured from one set of microlenses fabricated by a fixed combination of design and processing parameters as described. On the other hand, several other shapes of mold inserts including square and rectangle openings have been fabricated and tested to produce microlens arrays. For noncircular-shape openings, the top surfaces of the intruded plastic structures have irregular geometries such that it is difficult to characterize their optical properties. For the fabricated semi-spherical shape microlenses, the average  $f/\#$  is 0.88 with an average focal length of  $70.7 \mu\text{m}$ , aperture of  $80 \mu\text{m}$  when PC (the index of refraction of PC as 1.58) is used as the plastic material. On the other hand, it is important to characterize the radius of curvature of microlenses with respect to various micro intrusion conditions such as time, temperature and pressure and to predict the limitation of this process. Silicon mold inserts fabricated by a deep reactive ion etching process

have been utilized in the process characterization experiments instead of LIGA nickel mold inserts because silicon mold inserts can be easily fabricated for various trials. Differing from the experimental procedures used in the prototype fabrication process, the applied pressure is remained constant throughout the micro intrusion process in the silicon-mold-insert experiments and the processing pressure, temperature and time are recorded and characterized. The radius of curvature of the microlens is measured using an interferometer, Zygo Newview 5000 to obtain the surface profiles that are analyzed further by using the curve-fitting method on MATLAB. The best-fitted equation is used to calculate the curvature at each point and the mean radius of curvature is calculated accordingly. To verify the results from Zygo, one contour of the microlens surface is recorded in MATLAB as shown in Fig. 10 by importing a side view SEM image of a microlens. The lens surface appears to be a circular shape and the contour of the microlens can be fitted with an equation of a circle within 4% of variations across the lens surface. In the worst-case situation, it is estimated that the "deviation from spherical shape" is  $300 \text{ nm}$  among 95% of the lens surface.

The effect of processing time is first characterized by keeping the processing temperature at  $180^\circ\text{C}$  and processing pressure at  $0.8 \text{ MPa}$ . Fig. 11 shows the radius of curvature of microlenses under various processing time periods in the micro intrusion process on two sets of silicon holes of  $100 \mu\text{m}$  and  $200 \mu\text{m}$  in diameter, respectively. These empirical data suggest that the microlens radius of curvature decreases exponentially with time and the following expression is derived from the empirical data [18]:

$$R = R_1 + R_2 \exp\left(-\frac{t}{t_c}\right) \quad (6)$$

where  $R_1$  and  $R_2$  are radius constants depending on the size of opening and  $t_c$  is the time constant related to the size and

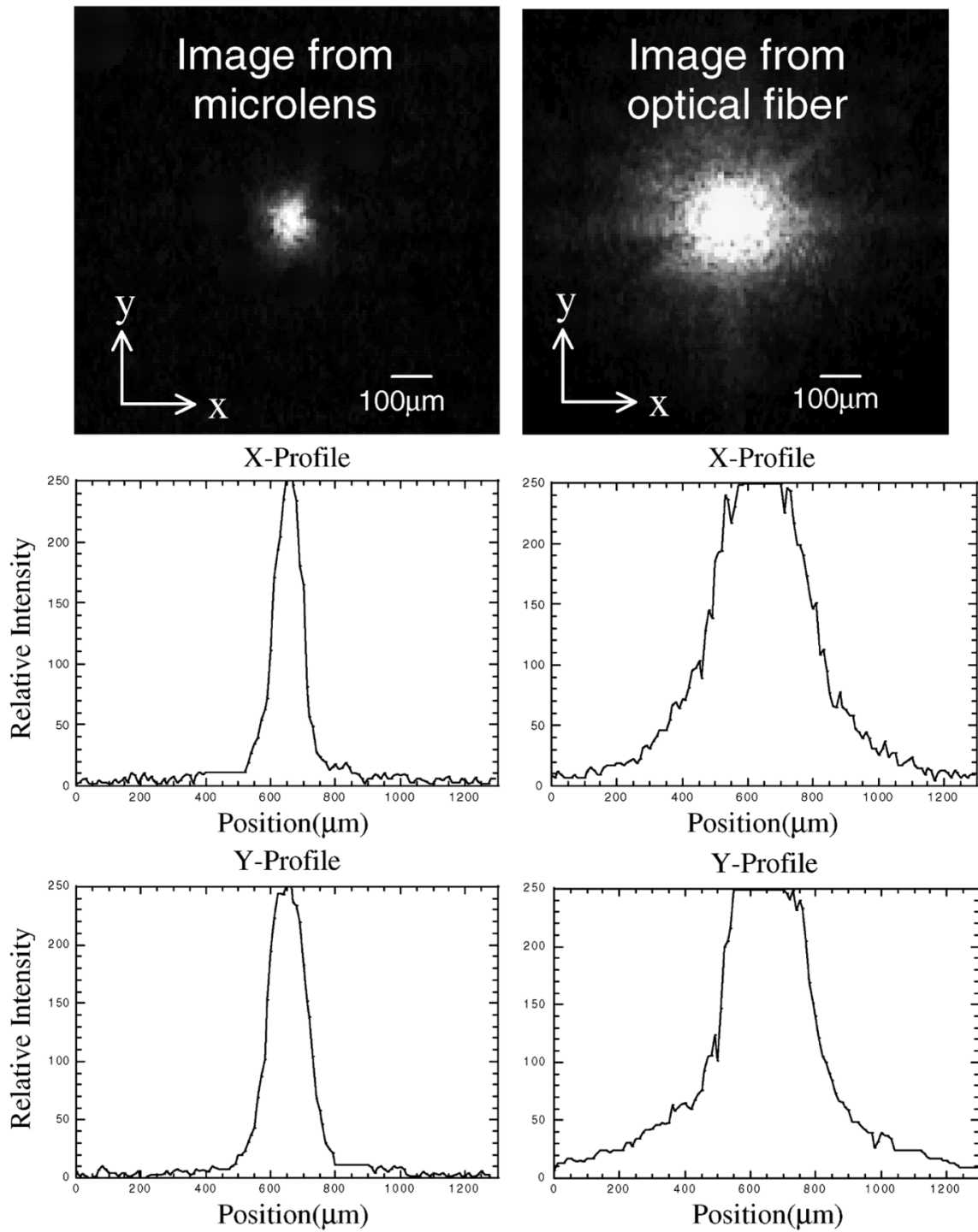


Fig. 9. Images and relative intensity from the optical fiber with (left) and without (right) the microlens (from the 80  $\mu\text{m}$  in diameter mold insert). These images are taken at the focal plane under an optical microscope by a CCD camera.

surface properties of openings and the material properties and processing conditions of the polymer material. The values of  $R_1$ ,  $R_2$ , and  $t_c$  are found to be 82  $\mu\text{m}$ , 113  $\mu\text{m}$  and 15 min for mold openings of 100  $\mu\text{m}$  in diameter; 146  $\mu\text{m}$ , 170  $\mu\text{m}$  and 10 min for mold openings of 200  $\mu\text{m}$  in diameter. In an analogy to the second order dynamic system, Fig. 11 suggests that the system is an over damped dynamic system and its settling time is proportional to the damping ratio of the system such that the intrusion process with smaller openings has longer settling time

to reach steady state [19]. Therefore, longer processing time for smaller openings is suggested to assure that steady state is reached to achieve the consistence of the fabrication process.

Investigation on the processing temperature is performed by fixing the processing time at 55 min (steady state) and processing pressure at 0.8 MPa. Fig. 12 shows the temperature dependent radius of curvature of microlens from 170  $^\circ\text{C}$  to 190  $^\circ\text{C}$ . A trend is observed that the radius of curvature reduces when the processing temperature increases probably due to the decrease

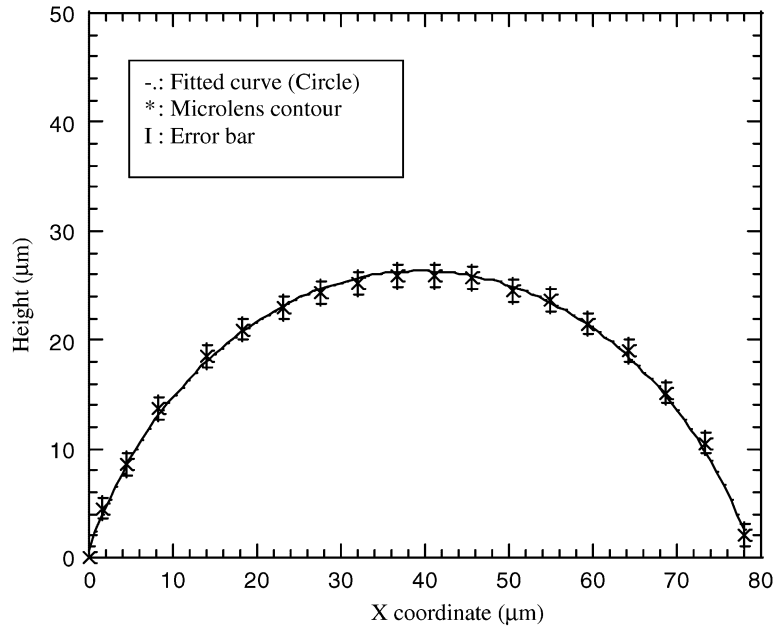


Fig. 10. The side-view SEM image (symbols) showing the top surface of the microlens (from the 80  $\mu\text{m}$  in diameter mold insert) as compared with a circular contour (solid line).

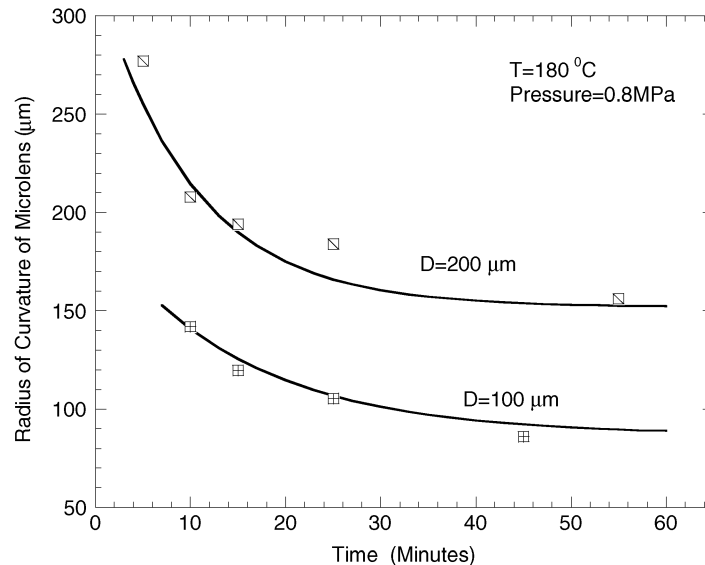


Fig. 11. Radius of curvature of microlens under various processing time periods in the micro-intrusion process.

of viscosity of polymer at higher temperature. The following Arrhenius-type function is proposed to describe the temperature dependent radius of curvature as an analogy to the viscosity changes with respect to temperature [18], [20]:

$$R = C_1 + C_2 \exp\left(\frac{\Delta H_R}{GT}\right) \quad (7)$$

where  $G$  is the universal gas constant (8.31 J/K·mol) and  $\Delta H_R$  is the activation energy. The value of  $\Delta H_R$  is experimentally determined by the curve fitting method as 5.18 kJ/mol for both mold openings of 100 and 200  $\mu\text{m}$  in diameter because the activation energy is a material related property that is independent of processing conditions. However,  $\Delta H_R$  may be different if

different material is used.  $C_1$  and  $C_2$  are constants depending on the size of the mold opening. Empirical curve fitting shows  $C_1 = -27 \mu\text{m}$ ,  $C_2 = 2.68 \mu\text{m}$  for the microlenses made from silicon openings of 100  $\mu\text{m}$  in diameter, and  $C_1 = -8.87 \mu\text{m}$ ,  $C_2 = 2.97 \mu\text{m}$  for the microlenses made from silicon openings of 120  $\mu\text{m}$  in diameter. This equation can help to design the desired radius of curvature of microlenses with the same size of openings by adjusting processing temperature but the values of  $C_1$ ,  $C_2$ , and  $\Delta H_R$  will change when different mold inserts and different materials are employed.

To investigate the effect of pressure variations with respect to the radius of curvature, the processing temperature is fixed at 180  $^{\circ}\text{C}$  and processing time is fixed at 55 min. Fig. 13 shows the radius of curvature with respect to the pressure variations.

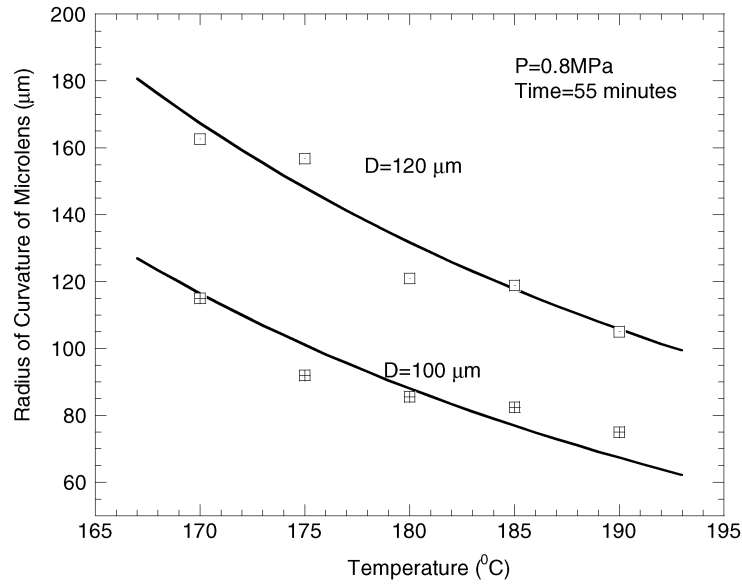


Fig. 12. Radius of curvature of microlens under various processing temperature in the micro intrusion process

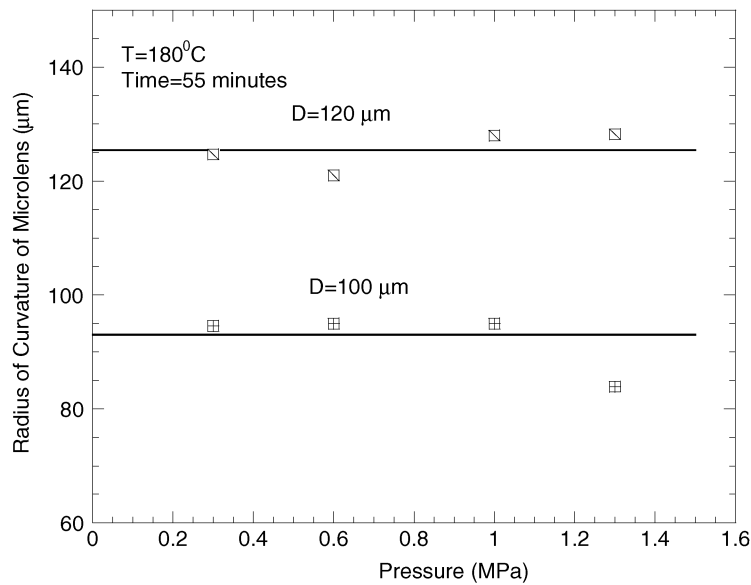


Fig. 13. Radius of curvature of microlens under different pressure in the micro-intrusion process.

The radius of curvature seems to remain the same with a variation of less than 5 μm under various levels of applied pressure. It can be concluded that pressure has little effect on the radius of curvature of the microlenses. However, if the applied pressure is too high, the top of the microlens may touch with the silicon substrate and become a flat surface such that maximum allowed pressure should be characterized for any specific intrusion process.

Another important parameter is the height of the microlens (the full height of the spherical lens and the pillar base) and its relationship with respect to the processing time, temperature and pressure. The characterization results [18] are summarized. First, it is found that the height of microlens reaches steady state when the radius of curvature reaches steady state. Second, the height of the microlens increases when the processing temperature increases and an Arrhenius function can be used to describe

the empirical data between the height and processing temperature. This result is similar to the characterizations of the radius of curvature of the microlens with respect to temperature, although different constants are extracted from the empirical data. Third, a close to linear relation between the height and the applied pressure is observed experimentally. The possible explanation is that when steady state is reached, the higher applied pressure results in more plastic material intruded into the mold insert and the depth is the result for balancing the applied pressure.

The above characterization helps drawing the following conclusions. It is possible to establish a stable micro-intrusion process that will be conducted at an elevated temperature (higher than the glass transition point of the polymer material) for sufficient time to assure that steady state is reached. As a result, the steady state radius of curvature and height of the microlenses are achieved and arrays of microlenses can be

fabricated with similar geometry and the standard deviation is small. The radius of curvature of the microlens is dominated by the processing temperature and the applied pressure has little effect. On the other hand, the height of the microlens can be controlled by the magnitude of the applied pressure and a linear relationship is expected. However, higher processing temperature will also result in the increase of the height of the microlens. Although the trends of the general processing parameters have been characterized, detail scientific investigations on the formation of the microlens and the processing conditions of the micro-intrusion process including possible density variations within the microlenses and the effects to the fluctuations in refractive index can be very challenging. These may include analyzes on complicated viscous flow of polymer material above the glass transition point in the micro scale, material and surface properties of the polymer and mold insert with respect to temperature variations and optical effects after the completion of the intrusion process. Other important factors such as reproducibility, lens lifetime and lens aberrations are also important and require further studies. The specific lens dimension could be reproduced under strictly controlled manufacturing conditions. Based on these experimental results, the maximum and minimum radii of curvature of fabricated microlenses are 280 and 90  $\mu\text{m}$  (the diameter of the openings holes are from 100 to 200  $\mu\text{m}$ ) and the  $f/\#$  is between 1.37 to 2.41.

## V. CONCLUSION

Microlens array fabricated by a micro-intrusion process has been successfully demonstrated by using polycarbonate as the processing material. This process provides an alternative way to manufacture microlenses with naturally formed lens surface. The fabricated microlens has a radius of curvature of  $41.4 \pm 1.05 \mu\text{m}$  under the standard intrusion process conditions of 0.6 MPa and 170 °C using a LIGA mold insert with the hole opening diameter of 80  $\mu\text{m}$ . A series of experiments is conducted to characterize the radius of curvature of microlenses with respect to processing time, temperature and pressure. It is found that intrusion processes with larger openings reach steady state faster than those with smaller openings. Furthermore, temperature dependent viscosity plays an important role in the micro-intrusion process to control the radius of curvature of the microlens. Analytically, the concept of  $\Delta H$  (the activation energy) and Arrhenius-type relationship is used for the first order approximation on the radius of curvature with respect to temperature and the activation energy is found to be 5.18 KJ/mole experimentally for polycarbonate in silicon mold insert. On the other hand, the effect of applied pressure on the radius of curvature of microlens is minimal. Further research is required to characterize the intrusion process analytically and experimentally when a new mold insert or other polymer materials are used to make microlenses.

## ACKNOWLEDGMENT

The authors wish to thank Dr. Y.-T. Cheng and R. Wilson for their help on taking SEM microphotos, B. Thronton and Prof. D. Bogy at the Department of Mechanical Engineering,

UC-Berkeley for their assistance on experimental measurements and Dr. J.-H. Tsai and Dr. Y.-C. Su for insightful discussions.

## REFERENCES

- [1] P. Ruther, B. Gerlach, J. Gottert, M. Ilie, J. Mohr, A. Muller, and C. Obmann, "Fabrication and characterization of microlenses realized by a modified LIGA process," *Pure Appl. Opt.*, vol. 6, no. 6, pp. 643–653, 1997.
- [2] H. Sankur, E. Motamedi, R. Hall, W. J. Gunning, and M. Khoshnevisan, "Fabrication of refractive microlens arrays," in *Proc. SPIE, Micro-Optics/Micromechanics and Laser Scanning and Shaping*, vol. 2383, 1995, pp. 179–183.
- [3] C. King, L. Lin, and M. Wu, "Out-of-plane refractive microlens fabricated by surface micromachining," *IEEE Photon. Technol. Lett.*, vol. 8, pp. 1349–1351, Oct. 1996.
- [4] U. Kohler, A. E. Guber, W. Bier, W. Hecke, and Th. Schaller, "Fabrication of microlenses by plasmaless isotropic etching combined with plastic moulding," *Sens. Actuators*, vol. A53, pp. 361–363, 1996.
- [5] H. W. Lau, N. A. Davies, and M. McCormick, "Microlens array fabricated in surface relief with high numerical aperture," *Proc. SPIE*, vol. 1544, pp. 178–188, 1991.
- [6] MEMS Optical [Online]. Available: <http://www.memsoptical.com>
- [7] M. Kufner and S. Kufner, *Micro-Optics and Lithography*, Brussels: VUBPRESS, 1997.
- [8] H. P. Herzig, *Micro-Optics Elements, Systems, and Applications*. Bristol, PA: Taylor and Francis, 1997.
- [9] S. Sinzinger and J. Jahns, *Microoptics*, 2nd ed. New York: Wiley, 2003.
- [10] L. Lin, T. K. Shia, and C.-J. Chiu, "Silicon-processed plastic micropyrramids for brightness enhancement applications," *J. Micromech. Microeng.*, vol. 10, no. 3, pp. 395–400, 2000.
- [11] L. Lin, C. J. Chiu, W. Bacher, and M. Hecke, "Microfabrication using silicon mold inserts and hot embossing," in *Proc. Seventh International Symposium on Micro Machine and Human Science*, 1996, pp. 67–71.
- [12] A. Picard, W. Ehrfeld, H. Lowe, H. Muller, and J. Schulze, "Refractive microlens arrays made by contactless embossing," *Proc. SPIE*, vol. 3135, pp. 96–105, 1997.
- [13] D. Koester, R. Mahedevan, and K. Marcus, *Multi-User MEMS Processes (MUMPS) Introduction and Design Rules*. NC: MCNC MEMS Technology Applications Center, 3021 Cornwallis Road, Research Triangle Park, Oct. 1994. rev. 3.
- [14] L. Lin, Y. T. Cheng, and C.-J. Chiu, "Comparative study of hot embossed microstructures fabricated by laboratory and commercial environments," *Microsyst. Technol. J.*, vol. 4, no. 3, pp. 113–116, 1998.
- [15] J. W. Blaker and W. M. Rosenblum, *Optics; An Introduction for Students of Engineering*. New York: Macmillan, 1993.
- [16] F. A. Jenkins and H. E. White, *Fundamentals of Optics*. New York: McGraw-Hill, 1957.
- [17] The MathWorks, Inc., Natick, MA.
- [18] X. Shen and L. Lin, "Micro plastic embossing process: experimental and theoretical characterizations," in *Proc. International Conference on Solid-State Sensors and Actuators*, vol. 2, 2001, pp. 1640–1643.
- [19] B. C. Kuo, *Automatic Control Systems*. Englewood Cliffs, NJ: Prentice Hall, 1995.
- [20] F. Yang, "Viscosity measurement of polycarbonate by using a penetration viscometer," *Polymer Eng. Sci.*, vol. 37, pp. 101–104, 1997.



**Li-Wei Pan** (M'02) was born in Taiwan, R.O.C. He received the B.S. degree in mechanical engineering from the National Chiao-Tung University, Hsinchu, Taiwan, R.O.C., in 1991, and the M.S. and Ph.D. degrees in mechanical engineering from The University of Michigan, Ann Arbor, in 1996 and 2001, respectively.

From 2002 to 2004, he was with Alza Corporation (a Johnson and Johnson company) working as a Research Engineer. In 2004, he joined Perkin Elmer, Inc. as a Mechanical Engineer. His research interests include micro drug delivery systems, microfluidic systems, IC and MEMS integration, LIGA microsensors and microactuators, and he has one U.S. patent pending.



**Xinjiang Shen** received the B.S. degree from Xi'an Jiaotong University, the M.S. degree from University of Houston, TX, and is currently working towards the Ph.D. degree in mechanical engineering at University of California, Berkeley.

Currently, he is a member of Computer Mechanics Laboratory, working on nanofluidics, particle flow contaminations and air bearing slider designs in hard-disk drives.



**Liwei Lin** (M'93) received the M.S. and Ph.D. degrees in mechanical engineering from the University of California, Berkeley, in 1991 and 1993 respectively.

From 1993 to 1994, he was with BEI Electronics, Inc. USA, working in microsensors research and development. From 1994 to 1999, he was an Associate Professor in the Institute of Applied Mechanics, National Taiwan University, Taiwan, and later an Assistant Professor at the Mechanical Engineering and Applied Mechanics Department at the University of

Michigan. He joined the University of California at Berkeley in 1999 and is now an Associate Professor at Mechanical Engineering Department and Co-Director at Berkeley Sensor and Actuator Center, NSF/Industry/University research cooperative center. His research interests are in design, modeling and fabrication of microstructures, microsensors and microactuators as well as mechanical issues in microelectromechanical systems and he holds 8 U.S. patents.

Dr. Lin is the recipient of the 1998 NSF CAREER Award for research in MEMS Packaging and the 1999 *ASME Journal of Heat Transfer* best paper award for his work on microscale bubble formation and is a subject editor for both the IEEE/ASME JOURNAL OF MICROELECTROMECHANICAL SYSTEMS and *Sensors and Actuators Journal*. He is the founding chairman of the MEMS division in ASME since 2004 and a Member of the American Society of Mechanical Engineers (ASME).